HHS Public Access

Author manuscript

J Biomech. Author manuscript; available in PMC 2016 May 01.

Published in final edited form as:

J Biomech. 2015 May 1; 48(7): 1325–1330. doi:10.1016/j.jbiomech.2015.03.009.

Hemodynamic Study of TCPC Using In Vivo and In Vitro 4D Flow MRI and Numerical Simulation

Alejandro Roldán-Alzate, PhD[1], **Sylvana García-Rodríguez, PhD**[1], **Petros V. Anagnostopoulos, MD**[3], **Shardha Srinivasan, MD**[3], **Oliver Wieben, PhD**[1,4], and **Christopher J. François, MD**[1]

[1]Department of Radiology, University of Wisconsin-Madison, USA

[2]Department of Pediatric Cardiothoracic Surgery, University of Wisconsin-Madison, USA

[3]Department of Pediatric Cardiology, University of Wisconsin-Madison, USA

[4]Department of Medical Physics, University of Wisconsin-Madison, USA

Abstract

Altered total cavopulmonary connection (TCPC) hemodynamics can cause long-term complications. Patient-specific anatomy hinders generalized solutions. 4D Flow MRI allows in vivo assessment, but not predictions under varying conditions and surgical approaches. Computational fluid dynamics (CFD) improves understanding and explores varying physiological conditions. This study investigated a combination of 4D Flow MRI and CFD to assess TCPC hemodynamics, accompanied with in vitro measurements as CFD validation. 4D Flow MRI was performed in extracardiac and atriopulmonary TCPC subjects. Data was processed for visualization and quantification of velocity and flow. Three-dimensional (3D) geometries were generated from angiography scans and used for CFD and physical model construction through additive manufacturing. These models were connected to a perfusion system, circulating water through the vena cavae and exiting through the pulmonary arteries at two flow rates. Models underwent 4D Flow MRI and image processing. CFD simulated the in vitro system, applying two different inlet conditions from in vitro 4D Flow MRI measurements; no-slip was implemented at rigid walls. Velocity and flow were obtained and analyzed. The three approaches showed similar velocities, increasing proportionally with high inflow. Atriopulmonary TCPC presented higher vorticity compared to extracardiac at both inflow rates. Increased inflow balanced flow distribution in both TCPC cases. Atriopulmonary IVC flow participated in atrium recirculation, contributing to RPA outflow; at baseline, IVC flow preferentially travelled through the LPA. The

Corresponding author: Alejandro Roldán-Alzate, PhD., WIMR Building, 1111 Highland Avenue, Madison, WI 53705, Phone: (608)262-1780, Fax: (608)263-0876, roldan@wisc.edu.

Conflict of Interest Statement

The authors state that there are no conflicts of interest related to this research study.

combination of patient-specific in vitro and CFD allows hemodynamic parameter control, impossible in vivo. Physical models serve as CFD verification and fine-tuning tools.

Keywords

total cavopulmonary connection; 4D Flow; magnetic resonance imaging; numerical simulation; additive manufacturing; congenital heart disease

1. Introduction

The incidence of single ventricle defects is 85 per million live births (Hoffman et al., 2004), and is considered a severe disease even after surgery. Treatment involves a series of surgeries, finalizing with a total cavo-pulmonary connection (TCPC), where the existing ventricle pumps blood to the systemic circulation and venous return passively enters the lungs via atriopulmonary or extracardiac connections. After finding right atrium-related complications of atriopulmonary connections in the 1990's, extracardiac procedures received more attention (Lardo et al., 1999). These were found to be more hemodynamically efficient and technically simpler. Nevertheless, atriopulmonary TCPC patients are the subject of follow-up and surgical revision studies.

Despite high initial survival rates, long-term performance gradually deteriorates (Dubini et al., 1996; Jayakumar et al., 2004; Lee et al., 2003; Marino, 2002). Complications include pulmonary arteriovenous malformation, systemic ventricular dysfunction, arrhythmia, decreased exercise capacity and thromboembolism. Assessments based on echocardiography and catheterization do not always correlate with functional status, and patient-specific anatomical complexity hinders the development of general procedures for all patients (AboulHosn et al., 2007; Pike et al., 2004; Stamm et al., 2002). A hemodynamically more efficient TCPC may lead to longer, event-free survival. Flow must meet systemic perfusion requirements, and caval pressures must overcome pulmonary vascular resistance. Vortical flow requires higher energy expenditure from the heart; in addition, recirculation and stagnation regions promote clot formation. Also, pulmonary artery flow distribution in balance is an important cause of arteriovenous malformations.

Due to flow complexity, single-directional ultrasound velocity measurements or two-dimensional (2D) Flow MRI remain limited in their ability to fully characterize TCPC flow. Four-dimensional (4D) Flow MRI captures three-directional velocity throughout the cardiac cycle. Although it offers valuable hemodynamic data, parameters such as flow rate, heart rate and vascular resistance, among others, cannot be varied in vivo, and therefore does not allow for predictive studies. For example, hemodynamic behavior during exercise cannot be assessed with MRI: heart rate cannot be voluntarily increased during scans.

There has been increasing interest in numerical and physical TCPC circulation models to improve our understanding of factors leading to complications and fatalities (Dasi et al., 2008; Ding et al., 2013; Dur et al., 2010; Haggerty et al., 2012a; Haggerty et al., 2012b; Haggerty et al., 2013; Kanter et al., 2012; KrishnankuttyRema et al., 2008; Soerensen et al., 2004; Venkatachari et al., 2007; Whitehead et al., 2007). While computational fluid

dynamics (CFD) provides powerful insights, the potential for predicting hemodynamics under different conditions and the ability of simulating different surgical procedures, it is currently not clinically used. In our experience, this is due to a lack of confidence on results; additional work is needed to confirm the accuracy of current CFD approaches or identify and address current shortcomings.

The purpose of this study was to assess TCPC hemodynamics using 4D Flow MRI in patients (in vivo), in patient-specific physical (in vitro) models and CFD simulations. In vitro physical models serve as a means 1) to control parameter variations and study their effects on hemodynamics, impossible to achieve in vivo, and 2) to compare in vitro velocity, measured with 4D Flow MRI, with that calculated by its CFD model. A deeper TCPC hemodynamics understanding might help identify early deterioration and intervene in an asymptomatic phase, increasing the operation's life span.

2. Methods

A summary of the sequence of events for the in vivo, in vitro and CFD analysis of TCPC is presented in Figure 1.

2.1. Subjects

MRI data from an IRB-approved and HIPAA-compliant protocol was retrospectively used. Data from two TCPC subjects, one with extracardiac TCPC (8-year-old male) and one with atriopulmonary TCPC (32-year-old female), were included (Figure 2). In the first case, the inferior vena cava (IVC) and superior vena cava (SVC) directly connect to the right and left pulmonary arteries (RPA and LPA, respectively). In atriopulmonary TCPC, blood enters a still-remaining cardiac cavity before flowing through the PA's. ah pues

2.2. MRI acquisition

4D Flow MRI was performed in each subject using Phase Contrast with Vastly undersampled Isotropic Projection Reconstruction (PC VIPR) (Johnson and Markl, 2010). Imaging parameters, in a clinical 3.0T scanner (MR750, GE Healthcare, Waukesha, WI), were: scan time: ~10 minutes, free breathing; imaging volume (FOV): 32×32×24 cm; 1.25 mm acquired isotropic spatial resolution; TR/TE = 6.4/2.2 ms; VENC = 100 cm/s and 200 cm/s for baseline and high inflow, respectively. A higher VENC for higher velocity avoided signal aliasing. A reconstruction with 20 frames per cardiac cycle was used for the in vivo dataset. Time-averaged reconstruction was used for in vitro 4D Flow MRI scans (Landgraf et al., 2014). Parameters for in vitro models, described hereafter, were exactly the same as those for in vivo imaging.

2.3. Anatomy segmentation

Anatomy segmentation of each subject was performed (Mimics; Materialise, Leuven, Belgium), where a three dimensional (3D) geometry was generated from the PC MR angiogram obatined from 4D Flow MRI. A supporting software, 3-matic, was used to smooth the geometry, fix surface defects and discretize it in tetrahedral elements while controlling element quality. The geometry was exported (STereoLithography, STL, format)

for fabrication of a physical model, and the mesh was exported (Fluent mesh) for numerical simulation.

2.4. 4D Flow MRI Analysis

4D Flow MRI scans were analyzed in a flow visualization package (EnSight, CEI Inc, Apex, NC). Quantitative flow analysis was conducted by placing cut-planes perpendicular to the vessel axis (SVC, IVC, RPA and LPA). Data from cut-planes were then analyzed in a Matlab-based tool (Mathworks, Naticks, MA) (Stalder et al., 2008). Average flow was obtained for all cut-planes; velocity streamlines were generated to visualize flow trajectories and have an insight on the velocity field.

2.5. Physical models: in vitro system

The TCPC 3D exported geometries were used to fabricate physical models to scale using selective laser sintering (SLS), an additive manufacturing technique for low-volume production of prototype models, which uses a high-power laser to fuse small polymer particles into a custom 3D shape. The SLS equipment (DTM Sinterstation 2500Cl ATC, 3D Systems, Inc., Rock Hill, SC, USA) was set up with laser power 12 W, scan spacing 0.15 mm, beam speed 5080 mm/s, and nylon 11 powder.

Physical models were connected to a perfusion system (Stockert SIII Heart-Lung Machine) (Figure 3), where water continuously entered the vena cavae (steady flow) and exited through the pulmonary arteries at two inflow rates: baseline (1 L/min and 3 L/min for the extracardiac and atriopulmonary TCPC, respectively) and high inflow (1.8 L/min and 4.5 L/min for the extracardiac and atriopulmonary TCPC, respectively). The model and tubing were set up on the scanner bed, imaged with in vivo scanning parameters and processed as described above. The three-directional velocity distributions were obtained at inlet planes, which had homogeneously distributed nodes. This data was exported for CFD model input.

2.6. Numerical models

A volumetric mesh of approximately 500,000 tetrahedral elements was exported for CFD (Fluent, ANSYS Inc., Canonsburg, PA), representing the fluid domain. Properties for water were defined (density: 1000 kg/m^3, viscosity: 0.001 Pa*s), simulating the in vitro system. Two different inlet conditions were implemented. First, an average normal velocity was defined, obtained from dividing the flow rate by the cross sectional area. Second, velocity fields of the three orthogonal components at the venae cavae, based on in vitro 4D Flow MRI velocity measurements, were extracted. After alignment of CFD model and in vitro inlet planes, constant interpolation was applied, where the velocity at CFD nodes was obtained from the nearest 4D Flow node. Baseline and high inflow were both simulated for the two TCPC models. Zero pressure was implemented at the outlets; no-slip boundary conditions were assigned on the walls, assumed to be rigid in accordance with physical models.

3. Results

For the extracardiac TCPC, vessel diameters were 13.6, 15.6, 5.82 and 9.31 mm for the SVC, IVC, LPA and RPA, respectively. For the atriopulmonary TCPC, vessel diameters were 12.2, 22.1, 12.1 and 14.6 mm for the SVC, IVC, LPA and RPA, respectively. The four vessels presented laminar and transitional flow regimes, where average Reynolds numbers (Re) were 1000 and 2400 for in vitro extracardiac baseline and high inflow, respectively. For the atripulmonary in vitro case, average Re were 2000 and 2300 for baseline and high inflow, respectively.

Color-coded velocity and distribution streamlines based on (1) in vivo measurements, (2) in vitro studies and (3) CFD calculations (in silico) are presented in Figures 4 and 5 for extracardiac and atriopulmonary TCPC, respectively. The latter illustrates the complex flow and helical patterns within the cardiac cavity, implying a much lower efficiency when compared to the extracardiac TCPC. Both cases demonstrate flow acceleration at the PA's. Relatively high velocity is present at the SVC. Satisfactory agreement is found between the three, especially between the in vitro and CFD models, as expected.

Quantitative flow measurements are summarized in Table 1, showing the flow distribution between the two PA's. Results from velocity component inlet boundary conditions were closer to in vitro measurements when compared to the model using average normal velocity inlet.

4. Discussion

Two TCPC cases were analyzed non-invasively using 4D Flow MRI. Establishing a pathway of further understanding patient-specific TCPC hemodynamics, and its effects from flow parameter variations, an in vitro system was developed using patient-specific physical models. This serves as a tool to not only control flow parameters but also to compare with CFD simulations.

MRI has previously been used to study TCPC hemodynamics. Be'eri et al. quantified TCPC flow, comparing different surgical approaches with multidimensional phase-velocity MRI (Be'eri et al., 1998). Data were averaged from multiple cardiac and respiratory cycles. Bächler et al. studied PA flow distribution from each vena cavae in TCPC subjects using 4D Flow MRI (Bachler et al., 2013). These studies, however, do not predict hemodynamics with physiological or anatomical changes, which is possible with CFD. Several groups have used CFD to demonstrate the geometry's role in TCPC hemodynamics (Dasi et al., 2009; Figliola et al., 2010; Kim et al., 1995; Sharma et al., 1996). Advances in computational power and medical imaging have allowed implementation of patient-specific data (de Zélicourt et al., 2010). There are still limitations in extending findings from numerical simulations to predicting long-term outcomes in TCPC patients (Dasi et al., 2009; Dasi et al., 2008; de Zélicourt et al., 2010).

The combination of in vitro 4D Flow MRI and CFD provides the potential to understand and predict hemodynamics in a controlled setting. In this study, an in vitro system incorporating patient-specific phantoms was used to vary inflow and study the resulting effects on the

velocity distribution, measured with 4D Flow MRI. This system was simulated with CFD, and the calculated velocity field from the simulation was compared with that measured in the in vitro system. The closer CFD results are to 4D Flow MRI measurements in the physical model, the more confidence is gained on the methodologies used to implement CFD boundary conditions to then simulate in vivo flow. Measurements with 4D Flow MRI could be compared with CFD, but not in the case of predictive studies. Thus, the in vitro system with patient-specific physical models establishes a bridge between in vivo 4D Flow MRI and high-confidence CFD models. Flow parameters can be varied and systematically analyzed, and geometric implications can be explored through additive manufacturing techniques. This is advantageous for visualization, surgical planning and TCPC optimization studies.

Improvements on the in vitro system are to be considered addressing flow artifacts at the tubing-model junction and tubing configuration. This issue might be related to the slight helicity demonstrated in Figures 4 and 5. A fixture, currently under development, will hold the tubing in place at an optimal position. Future plans include instrumentation of the in vitro system to obtain direct measurements of pressure and flow and to have the ability to control the vascular resistance.

The assumption of rigid walls is recognized as an inaccuracy factor in cardiovascular CFD. However, the purpose of this study was to simulate the in vitro system, involving a rigid physical model, and not the in vivo scan. Initial assumptions of rigid walls allow a means of further understanding and decomposing TCPC hemodynamic phenomena, isolating the non-linear effect of viscoelastic vessel walls from anatomical and inlet flow factors. This results in a more physiological model, better representing patient-specific conditions. Physical models are rigid, but pilot studies are under way using other SLS materials, such as thermoplastic elastomers, more closely resembling vessel walls.

Successful correlation of in vivo 4D Flow MRI and validated CFD will provide a powerful non-invasive surveillance tool that will allow clinicians to follow TCPC performansice over time, to identify potential hemodynamic deterioration and intervene in asymptomatic phases to increase TCPC life span. Patient-specific physical models with in vitro 4D Flow MRI measurements allow fine-tuning and verification of CFD models, thus providing an even higher accuracy of patient-specific CFD models and a lower gap between clinical implementation.

Acknowledgments

The authors are grateful to Leonardo Rivera, Department of Physics; Prof. Tim Osswald, Polymer Engineering Center, Department of Mechanical Engineering, University of Wisconsin-Madison and his research group. GE Healthcare provides support to MR research in the University of Wisconsin. This study was partially supported by an American Heart Association Scientist Development Grant (#14SDG19690010) awarded to Dr. Roldán-Alzate.

References

AboulHosn J, Danon S, Levi D, Castellon Y, Child J, Moore J. Regression of pulmonary arteriovenous malformations after transcatheter reconnection of the pulmonary arteries in patients with unidirectional Fontan. Congenital heart disease. 2007; 2:179–184. [PubMed: 18377462]

Bachler P, Valverde I, Pinochet N, Nordmeyer S, Kuehne T, Crelier G, Tejos C, Irarrazaval P, Beerbaum P, Uribe S. Caval blood flow distribution in patients with Fontan circulation: quantification by using particle traces from 4D flow MR imaging. Radiology. 2013; 267:67–75. [PubMed: 23297331]

Be'eri E, Maier SE, Landzberg MJ, Chung T, Geva T. In vivo evaluation of Fontan pathway flow dynamics by multidimensional phase-velocity magnetic resonance imaging. Circulation. 1998; 98:2873–2882. [PubMed: 9860790]

Dasi LP, Krishnankuttyrema R, Kitajima HD, Pekkan K, Sundareswaran KS, Fogel M, Sharma S, Whitehead K, Kanter K, Yoganathan AP. Fontan hemodynamics: importance of pulmonary artery diameter. The Journal of thoracic and cardiovascular surgery. 2009; 137:560–564. [PubMed: 19258065]

Dasi LP, Pekkan K, Katajima HD, Yoganathan AP. Functional analysis of Fontan energy dissipation. Journal of biomechanics. 2008; 41:2246–2252. [PubMed: 18508062]

de Zélicourt DA, Marsden A, Fogel MA, Yoganathan AP. Imaging and patient-specific simulations for the Fontan surgery: Current methodologies and clinical applications. Progress in Pediatric Cardiology. 2010; 30:31–44. [PubMed: 25620865]

Ding J, Liu Y, Wang F. Influence of bypass angles on extracardiac Fontan connections: a numerical study. International journal for numerical methods in biomedical engineering. 2013; 29:351–362. [PubMed: 23345174]

Dubini G, de Leval MR, Pietrabissa R, Montevecchi FM, Fumero R. A numerical fluid mechanical study of repaired congenital heart defects. Application to the total cavopulmonary connection. Journal of biomechanics. 1996; 29:111–121. [PubMed: 8839024]

Dur O, DeGroff CG, Keller BB, Pekkan K. Optimization of inflow waveform phase-difference for minimized total cavopulmonary power loss. Journal of biomechanical engineering. 2010; 132:031012. [PubMed: 20459200]

Figliola RS, Giardini A, Conover T, Camp TA, Biglino G, Chiulli J, Hsia TY. In Vitro Simulation and Validation of the Circulation with Congenital Heart Defects. Progress in pediatric cardiology. 2010; 30:71–80. [PubMed: 21218147]

Haggerty CM, de Zelicourt DA, Restrepo M, Rossignac J, Spray TL, Kanter KR, Fogel MA, Yoganathan AP. Comparing pre- and post-operative Fontan hemodynamic simulations: implications for the reliability of surgical planning. Annals of biomedical engineering. 2012a; 40:2639–2651. [PubMed: 22777126]

Haggerty CM, de Zélicourt DA, Restrepo M, Rossignac J, Spray TL, Kanter KR, Fogel MA, Yoganathan AP. Comparing pre- and post-operative Fontan hemodynamic simulations: implications for the reliability of surgical planning. Annals of biomedical engineering. 2012b; 40:2639–2651. [PubMed: 22777126]

Haggerty CM, Kanter KR, Restrepo M, de Zelicourt DA, Parks WJ, Rossignac J, Fogel MA, Yoganathan AP. Simulating hemodynamics of the Fontan Y-graft based on patient-specific in vivo connections. The Journal of thoracic and cardiovascular surgery. 2013; 145:663–670. [PubMed: 22560957]

Hoffman JI, Kaplan S, Liberthson RR. Prevalence of congenital heart disease. American heart journal. 2004; 147:425–439. [PubMed: 14999190]

Jayakumar KA, Addonizio LJ, Kichuk-Chrisant MR, Galantowicz ME, Lamour JM, Quaegebeur JM, Hsu DT. Cardiac transplantation after the Fontan or Glenn procedure. Journal of the American College of Cardiology. 2004; 44:2065–2072. [PubMed: 15542293]

Johnson KM, Markl M. Improved SNR in phase contrast velocimetry with five-point balanced flow encoding. Magnetic resonance in medicine : official journal of the Society of Magnetic Resonance in Medicine/Society of Magnetic Resonance in Medicine. 2010; 63:349–355.

Kanter KR, Haggerty CM, Restrepo M, de Zelicourt DA, Rossignac J, Parks WJ, Yoganathan AP. Preliminary clinical experience with a bifurcated Y-graft Fontan procedure--a feasibility study. The Journal of thoracic and cardiovascular surgery. 2012; 144:383–389. [PubMed: 22698555]

Kim YH, Walker PG, Fontaine AA, Panchal S, Ensley AE, Oshinski J, Sharma S, Ha B, Lucas CL, Yoganathan AP. Hemodynamics of the Fontan connection: an in-vitro study. Journal of biomechanical engineering. 1995; 117:423–428. [PubMed: 8748524]

KrishnankuttyRema R, Dasi LP, Pekkan K, Sundareswaran K, Fogel M, Sharma S, Kanter K, Spray T, Yoganathan AP. Quantitative analysis of extracardiac versus intraatrial Fontan anatomic geometries. The Annals of thoracic surgery. 2008; 85:810–817. [PubMed: 18291147]

Landgraf BR, Johnson KM, Roldan-Alzate A, Francois CJ, Wieben O, Reeder SB. Effect of temporal resolution on 4D flow MRI in the portal circulation. Journal of magnetic resonance imaging : JMRI. 2014; 39:819–826. [PubMed: 24395121]

Lardo AC, Webber SA, Friehs I, del Nido PJ, Cape EG. Fluid dynamic comparison of intra-atrial and extracardiac total cavopulmonary connections. The Journal of thoracic and cardiovascular surgery. 1999; 117:697–704. [PubMed: 10096964]

Lee JR, Choi JS, Kang CH, Bae EJ, Kim YJ, Rho JR. Surgical results of patients with a functional single ventricle. European journal of cardio-thoracic surgery : official journal of the European Association for Cardio-thoracic Surgery. 2003; 24:716–722. [PubMed: 14583304]

Marino BS. Outcomes after the Fontan procedure. Current opinion in pediatrics. 2002; 14:620–626. [PubMed: 12352258]

Pike NA, Vricella LA, Feinstein JA, Black MD, Reitz BA. Regression of severe pulmonary arteriovenous malformations after Fontan revision and “hepatic factor” rerouting. The Annals of thoracic surgery. 2004; 78:697–699. [PubMed: 15276554]

Sharma S, Goudy S, Walker P, Panchal S, Ensley A, Kanter K, Tam V, Fyfe D, Yoganathan A. In vitro flow experiments for determination of optimal geometry of total cavopulmonary connection for surgical repair of children with functional single ventricle. Journal of the American College of Cardiology. 1996; 27:1264–1269. [PubMed: 8609354]

Soerensen DD, Pekkan K, Sundareswaran KS, Yoganathan AP. New power loss optimized Fontan connection evaluated by calculation of power loss using high resolution PC-MRI and CFD. Conference proceedings : … Annual International Conference of the IEEE Engineering in Medicine and Biology Society. IEEE Engineering in Medicine and Biology Society. Conference. 2004; 2:1144–1147.

Stalder AF, Russe MF, Frydrychowicz A, Bock J, Hennig J, Markl M. Quantitative 2D and 3D phase contrast MRI: optimized analysis of blood flow and vessel wall parameters. Magnetic resonance in medicine : official journal of the Society of Magnetic Resonance in Medicine/Society of Magnetic Resonance in Medicine. 2008; 60:1218–1231.

Stamm C, Friehs I, Duebener LF, Zurakowski D, Mayer JE Jr, Jonas RA, del Nido PJ. Improving results of the modified Fontan operation in patients with heterotaxy syndrome. The Annals of thoracic surgery. 2002; 74:1967–1977. discussion 1978. [PubMed: 12643382]

Venkatachari AK, Halliburton SS, Setser RM, White RD, Chatzimavroudis GP. Noninvasive quantification of fluid mechanical energy losses in the total cavopulmonary connection with magnetic resonance phase velocity mapping. Magnetic resonance imaging. 2007; 25:101–109. [PubMed: 17222721]

Whitehead KK, Pekkan K, Kitajima HD, Paridon SM, Yoganathan AP, Fogel MA. Nonlinear power loss during exercise in single-ventricle patients after the Fontan: insights from computational fluid dynamics. Circulation. 2007; 116:I165–171. [PubMed: 17846299]

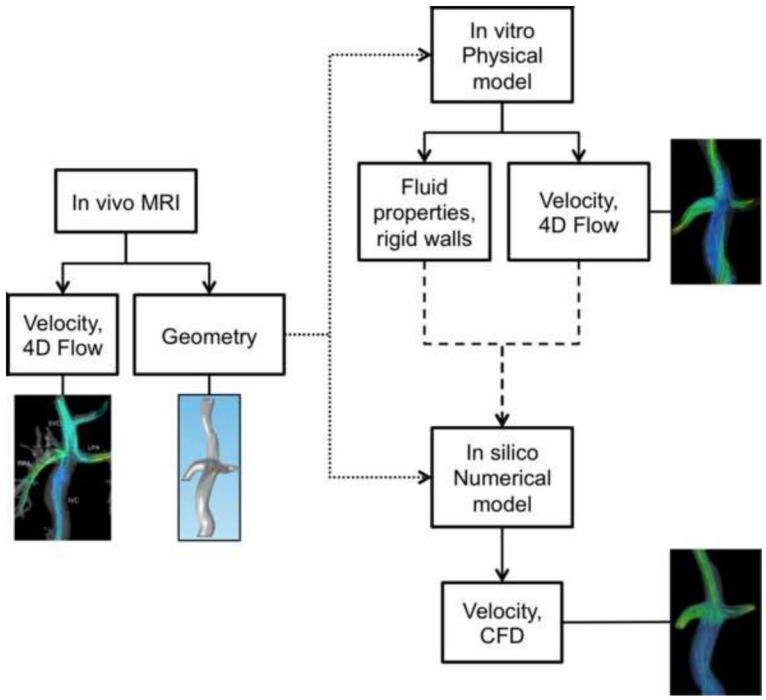

Figure 1.
Schematic description of the sequence of events in the analysis of TCPC.

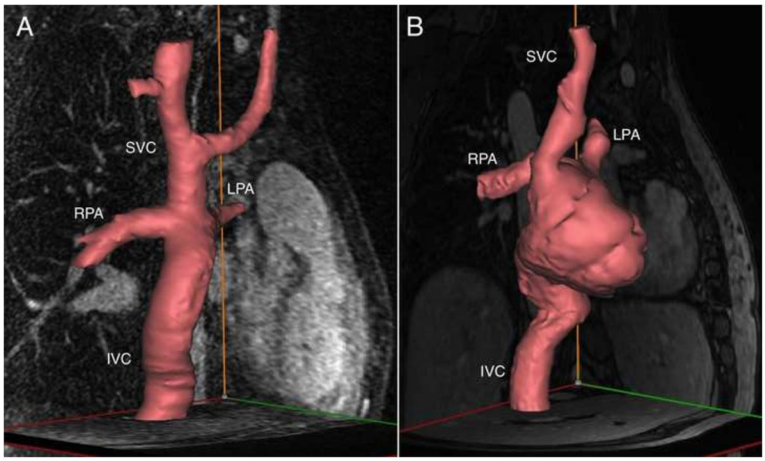

Figure 2.

Patient-specific three-dimensional models of the TCPC anatomy based on phase contrast magnetic resonance angiography scans. **A**) Extracardiac TCPC; **B**) Atriopulmonary TCPC.

Figure 3.

Physical models were connected to a perfusion system (**A**), which circulated water entering through the vena cavae and exiting through the pulmonary arteries as shown for the extracardiac TCPC case (**B**). The physical model and tubing were placed in the scanner (**C**) to assess fluid flow by means of 4D Flow MRI.

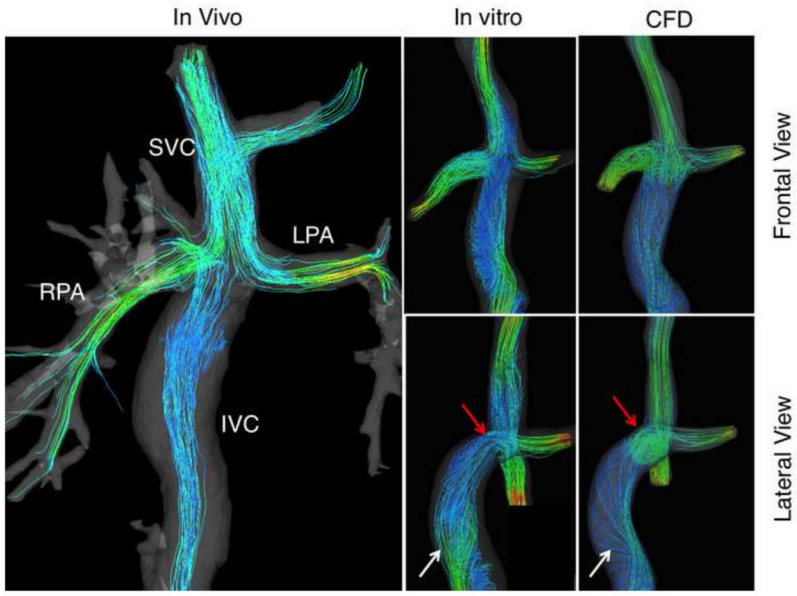

Figure 4.

Color-coded velocity and distribution streamlines showing the flow trajectory through the extracardiac TCPC obtained from in vivo and in vitro 4D Flow MRI, and calculated by means of CFD. White arrows in the lateral view show the vortical flow in the inferior vena cava (IVC) of the in-vitro and the CFD models. Red arrows reveal the vortex formation at the confluence of the IVC, superior vena cava (SVC), right pulmonary artery (RPA) and left pulmonary artery (LPA).

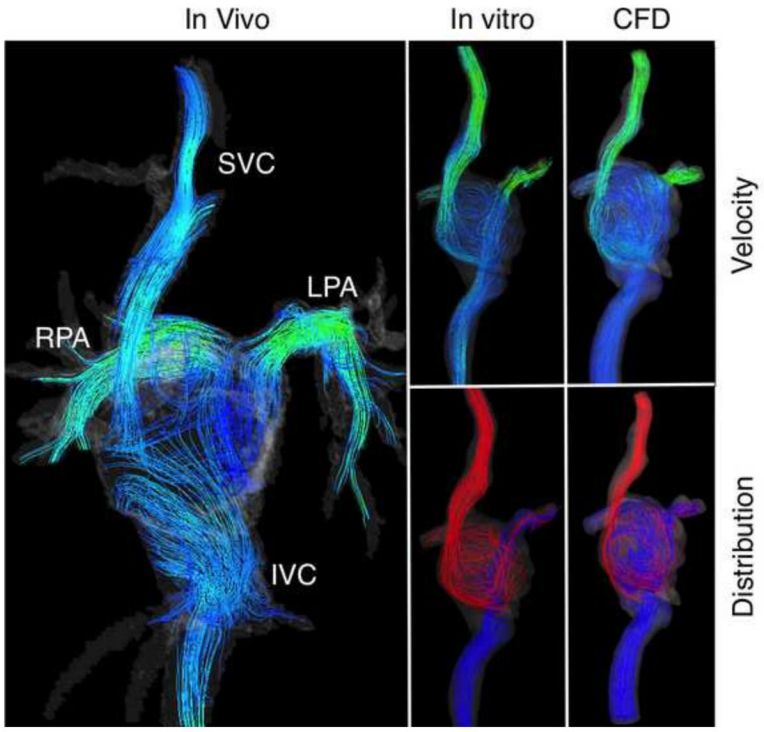

Figure 5.
Color-coded velocity and distribution streamlines showing the flow trajectory through the atriopulmonary TCPC obtained from in vivo and in vitro 4D Flow MRI, and calculated by means of CFD.

Table 1

In vivo and in vitro flow measurements and CFD simulations at cross sections of the main vessels. Flow ratios into each of the pulmonary arteries are presented for in vivo and in vitro experiments as well as for CFD simulations using velocity components (VC) and average normal inflow velocity (ANIV) at the inlet plane.

	Flow (L/min)		Flow ratio (VC)		Flow ratio (ANIV)	
	IVC	SVC	LPA	RPA	LPA	RPA
Extra in vivo	0.4	0.72	0.30	0.70		
Extra 1 Lt in vitro	0.59	0.38	0.45	0.55		
Extra 1 Lt CFD	0.61	0.39	0.32	0.68	0.71	0.29
Extra 1.8 Lt in vitro	1.26	0.63	0.45	0.55		
Extra 1.8 Lt CFD	1.32	0.48	0.48	0.52	0.48	0.52
Atrio In vivo	2.09	0.95	0.41	0.59		
Atrio 3 Lt in vitro	1.10	1.86	0.35	0.65		
Atrio 3 Lt CFD	1.05	1.95	0.40	0.60	0.71	0.29
Atrio 4.5 Lt in vitro	1.73	2.77	0.42	0.58		
Atrio 4.5 Lt CFD	1.87	2.63	0.41	0.59	0.50	0.50